Inertial range and the finite Reynolds number effect of turbulence

J. Qian
Department of Physics, Graduate School of Academia Sinica, P.O. Box 3908, Beijing 100039, China
(Received 31 May 1996)

The Kolmogorov $\frac{4}{5}$ law, which is the unique, exact relationship of inertial-range statistics, is applied to investigate the finite Reynolds number effect, in particular to study how the width of the inertial range of finite Reynolds number turbulence changes with the Taylor microscale Reynolds number R_λ. It is found that there is no inertial range when $R_\lambda \leqslant 2000$ and, within tolerance of 1% error, R_λ should be higher than 10^4 in order to have an inertial range wider than one decade. The so-called inertial range found in experiments and simulations is just a scaling range and is not the same as Kolmogorov's inertial range. The finite Reynolds number effect cannot be neglected within such a scaling range and should be considered in comparing experiments (or simulations) with theories of the inertial-range statistics. [S1063-651X(96)03112-1]

PACS number(s): 47.27.Gs, 47.27.Jv

The concept of inertial range proposed by Kolmogorov plays a central role in the statistical physics of turbulence [1,2]. The idealized model of inertial range corresponds to the asymptotic case of infinite Reynolds number, while field observations, laboratory experiments, and numerical simulations are made for turbulent flows at finite Reynolds numbers. It is commonly believed that when the Reynolds number is high enough, small-scale statistics within some small-scale range of finite Reynolds number turbulence can be described by the idealized model of the inertial range. In other words, the finite Reynolds number effect approaches zero as the Reynolds number becomes higher and higher. Of course, it might be possible that the finite Reynolds number effect persists while the Reynolds number approaches infinity (this possibility is not considered in this paper). In comparing experiments (or simulations) with theories, it is important to know quantitatively how fast the finite Reynolds number effect approaches zero as the Reynolds number becomes higher and higher. For example, it is interesting to know whether the Taylor microscale Reynolds number $R_\lambda = 800$ (or 1500) is high enough for the existence of a small-scale range within which the idealized inertial-range model is valid and the finite Reynolds number effect is negligible. Some say ''yes'' and some say ''no.''

A popular method to determine the inertial range of finite Reynolds number turbulence in experiments and simulations is to make a log-log plot of the one-dimensional (1D) longitudinal spectra against the wave number k to find a $k^{-5/3}$ range and then take this $k^{-5/3}$ range as the inertial range, or to take the $r^{2/3}$ range in a log-log plot of the second-order structure function $D_{LL}(r)$ against the distance r as the inertial range. For example, in their famous tidal experiments ($R_\lambda \approx 2000$), Grant, Stewart, and Moilliet [3] observed a $k^{-5/3}$ range of nearly three decades. More examples are shown in Fig. 9 of [4]. In fact, the viscous effect and the large-scale effect cannot be neglected within the scaling range observed in experiments and simulations, and the scaling range is not the same as Kolmogorov's inertial range. In this paper, the third-order structure function $D_{LLL}(r)$ is used to determine the inertial range and to study the difference between the inertial range and the scaling range because there is an exact inertial-range relationship for $D_{LLL}(r)$ (the Kolmogorov $\frac{4}{5}$ law [1]),

$$D_{LLL}(r) = -\tfrac{4}{5}\epsilon r, \tag{1}$$

where ϵ is the energy dissipation rate. Figure 1 gives $-D_{LLL}(r)/\epsilon r$ versus $\log_{10}(k_d r)$ of finite Reynolds number turbulence for $R_\lambda = 200$, 500, 1500, 10^4, and 10^5. Here $1/k_d = (\nu^3/\epsilon)^{1/4}$ is the Kolmogorov length scale. The method of calculating $D_{LLL}(r)$ is explained in the next two paragraphs. A log-log plot of $D_{LLL}(r)$ against r for $R_\lambda = 1500$ is given in Fig. 2, where $D_{LLL}(r)$ scales as r over about two decades, and this scaling range is commonly taken as the inertial range in experiments. However, Fig. 1 shows that $-D_{LLL}(r)/\epsilon r$ deviates from the inertial-range value 0.8 over the $D_{LLL}(r) \sim r$ scaling range shown in Fig. 2. According to Kolmogorov's $\frac{4}{5}$ law (1), $-D_{LLL}(r)/\epsilon r$ should be equal to 0.8 in the inertial range and the deviation of $-D_{LLL}(r)/\epsilon r$ from 0.8 implies that the viscous effect or the large-scale effect is not negligible. Therefore, strictly speaking, the $D_{LLL}(r) \sim r$ scaling ranges observed in experiments or simulations are not Kolmogorov's inertial range. In other words,

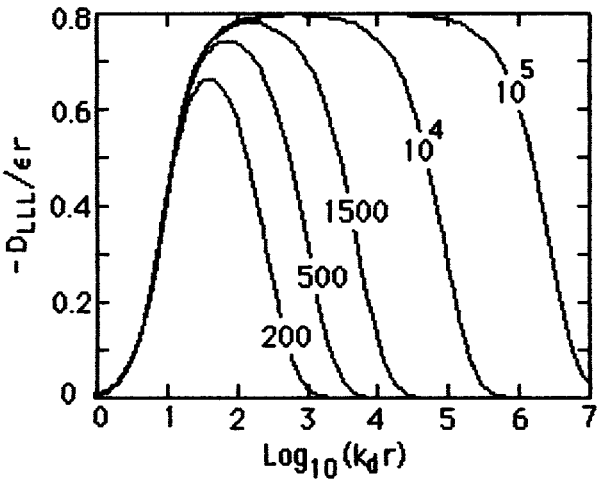

FIG. 1. $-D_{LLL}(r)/\epsilon r$ vs $\log_{10}(k_d r)$ of finite Reynolds number turbulence for $R_\lambda = 200$, 500, 1500, 10^4, and 10^5. k_d is the Kolmogorov wave number. Ko=1.5, $n=1$, and $\eta(k)$ is (10a).

 © 1997 The American Physical Society

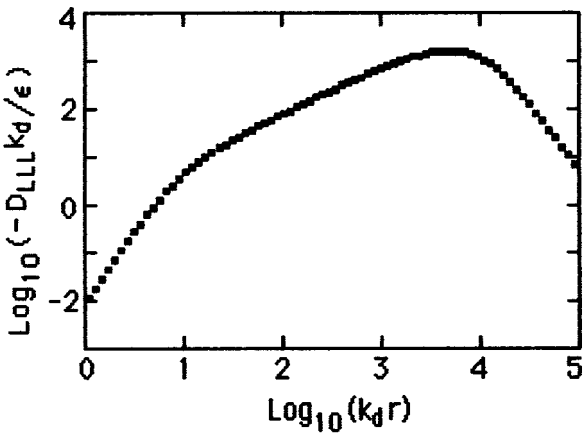

FIG. 2. $\mathrm{Log}_{10}[-D_{LLL}(r)k_d/\epsilon]$ vs $\log_{10}(k_d r)$ for $R_\lambda=1500$.

within the scaling ranges found in experiments or simulations, the finite Reynolds number effect is not negligible and has to be considered.

Before studying the finite Reynolds number effect in detail, we explain how to calculate the third-order structure function $D_{LLL}(r)$ of finite Reynolds number turbulence [readers not interested in the method of calculating $D_{LLL}(r)$ can skip the following two paragraphs]. By a similar process of deriving Eq. (12.141) of [1], we obtain

$$-D_{LLL}(r)=12\int_0^\infty T(x/r)[x^2\sin(x)+3x\cos(x) -3\sin(x)]/x^5 dx, \tag{2}$$

where $T(k)$ with $k=x/r$ is the energy transfer spectrum function. From (2) we have

$$-D_{LLL}(r)=\sum_{i=1}^{\infty}\left[C_{2i+1}\int_0^\infty T(k)k^{(2i)}dk\right]r^{(2i+1)}, \tag{3a}$$

$$C_3=\tfrac{2}{35}, \quad C_5=-C_3/36, \quad C_7=-C_5/66, \tag{3b}$$

etc. For small r, $D_{LLL}(r)$ can be calculated by using only first three terms of the series (3a). For larger r, the series (3a) might not be convergent; the integral (2) has to be used to calculate $D_{LLL}(r)$. While using (2) and (3) to calculate $D_{LLL}(r)$, $T(k)$ has to satisfy the energy relationship

$$\int_0^\infty T(k)dk=0. \tag{4}$$

Therefore, the problem of calculating $D_{LLL}(r)$ becomes how to determine the energy transfer spectrum function $T(k)$. Various statistical closure methods of the Navier-Stokes equation [5–8] yield the following expression for $T(k)$:

$$T(k)=16\pi^2k^3\int_0^\infty dr\, r\int_{\max(k-r,r)}^{k+r} dp\, p\, G(k,p,r)/[\eta(k) +\eta(p)+\eta(r)], \tag{5a}$$

$$G(k,p,r)=b(k,p,r)q(r)[q(p)-q(k)]+b(k,r,p)q(p) \times[q(r)-q(k)], \tag{5b}$$

$$q(k)=E(k)/4\pi k^2. \tag{5c}$$

Here $E(k)$ is the 3D energy spectrum,

$$b(k,p,r)=(p/k)(xy+z^3) \tag{5d}$$

is a geometrical factor, and x, y, and z are the cosines of three angles of the triangle with sides k, p, and r. The key of the closure problem [6] is how to determine $\eta(k)$, which has different meanings in different closure methods. For example, $\eta(k)$ represents the response function in Kraichnan's direct interaction approximation (DIA) closure [5,6], while [8] treats $\eta(k)$ as the optimal control parameter to minimize the error of the approximate solution of the Liouville equation of turbulence. It is easy to prove that the $T(k)$ given by (5) satisfies (4). Therefore, if $E(k)$ and $\eta(k)$ are known, we can use (5) to evaluate $T(k)$ and then use (2) or (3) to calculate $D_{LLL}(r)$. In the universal equilibrium range, $E(k)$ and $\eta(k)$ have to satisfy the spectral form of the von Kármán–Howarth equation for stationary turbulence

$$T(k)=2\nu k^2E(k). \tag{6a}$$

In the inertial range, the viscous effect is negligible (6a) become [1]

$$T(k)=0, \tag{6b}$$

and

$$\Pi(k)=\int_k^\infty T(k')dk'=\epsilon \tag{6c}$$

Here k is in the inertial range and $\Pi(k)$ is the energy transfer function.

In this paragraph, we explain how to determine $E(k)$ and $\eta(k)$ appearing in $T(k)$ of (5). In the inertial range, we have [8]

$$E(k)=\mathrm{Ko}\epsilon^{2/3}k^{-5/3}, \tag{7a}$$

$$\eta(k)=D\epsilon^{1/3}k^{2/3}, \tag{7b}$$

where Ko is the Kolmogorov constant, and by (5) and (6c) we obtain

$$\mathrm{Ko}^2/D=5.25, \tag{7c}$$

which does not depend upon which closure method is used. Different closure methods [5–8] predict different values of D^2/Ko and hence predict different Ko (and D). In order to avoid the issue of which closure method is better, we consider the Kolmogorov constant Ko as an adjustable parameter and D as determined by (7c), and then study how $D_{LLL}(r)$ depends upon Ko. As shown later, our conclusions do not depend upon which of the closure methods is used. In the universal equilibrium range, we have

$$E(k)=\mathrm{Ko}\epsilon^{2/3}k^{-5/3}F(k/k_d), \quad F(0)=1. \tag{8a}$$

According to Kolmogorov, $F(x)$ is a universal function of $x=k/k_d$; (8a) becomes (7a) in the inertial range. $F(x)$ decreases exponentially in the dissipation range. Hence, in

solving (6a) with (5) by the equation-error method [9], the following trial form of $F(x)$ is used:

$$F(x)=(1+Bx^{\alpha}g)\exp(-Cx^{\beta}), \tag{8b}$$

$$g=[1+C_1Z+C_2Z^2+\cdots+C_mZ^m]^2, \quad Z=x^{\gamma}. \tag{8c}$$

The parameter B, α, C, β, C_1, C_2, . . . , C_m, and γ are adjusted to make the equation error of (6a) as small as possible. These adjustable parameter have to satisfy the following constraint during the optimization computation:

$$\epsilon=2\nu\int_0^{\infty}E(k)k^2dk$$

or

$$2\mathrm{Ko}\int_0^{\infty}x^{1/3}F(x)dx=1. \tag{9}$$

When taking viscous effects into account, a reasonable form of $\eta(k)$ is [8,9]

$$\eta(k)=D\epsilon^{1/3}k^{2/3}+\nu k^2=\epsilon^{1/3}k^{2/3}[D+(k/k_d)^{4/3}], \tag{10a}$$

which becomes (7b) in the inertial range. An improved form of $\eta(k)$ is [9]

$$\eta(k)=\epsilon^{1/3}k^{2/3}[D+D_1(k/k_d)^{2/3}+(k/k_d)^{4/3}] \tag{10b}$$

and D_1 is also treated as adjustable parameter. All three forms of $\eta(k)$, i.e., (7b), (10a), and (10b), are tried in solving (6a) numerically to determine $F(x)$. Similar forms of $F(x)$ are obtained; in particular, we obtain $B>0$, implying the existence of a bump between the inertial range and the dissipation range. It will be shown later that our conclusions do not depend upon which form of $\eta(k)$ is used. Thirty sampling points over the range $10^{-3}<k/k_d<1$ are used in solving (6a) by the equation-error method (only two sampling points were used in [9]). The more terms in (8c) used, the better the optimal solution. When $m=5$ in (8c), the equation error of (6a) for the optimal solution is less than 0.002, which is good enough. As an illustration, Fig. 3 shows two optimal solutions of (6a) that satisfy (6a) very well and Fig. 4 shows the case of $F(x)$ being Pao's formula, which does not satisfy (6a). In the energy-containing range, (6a) is no longer valid; moreover, $E(k)$ is not universal. Within the framework of isotropic turbulence, the following model is commonly adopted [10] to extrapolate (8a) to the energy-containing range:

$$E(k)=\mathrm{Ko}\epsilon^{2/3}k^{-5/3}F(k/k_d)/[1+(k_0/k)^{n+5/3}]. \tag{11}$$

Here k_0 is the characteristic wave number of the energy-containing range and n represents how fast $E(k)$ decreases to zero as $k\to 0$ ($n=1$ is used in [10]). The wave-number ratio k_0/k_d is related to the Reynolds number R_λ. By definition,

$$R_\lambda=\langle u^2\rangle^{1/2}\lambda/\nu, \quad \lambda=[\langle u^2\rangle/\langle(\partial u/\partial x)^2\rangle]^{1/2},$$

u is the turbulent velocity component along the x direction, and $\langle\ \rangle$ denotes the statistical average. For isotropic turbulence, $\langle u^2\rangle=\frac{2}{3}\int_0^{\infty}E(k)dk$ and $\epsilon=15\nu\langle(\partial u/\partial x)^2\rangle$. By (11), after some manipulation we have

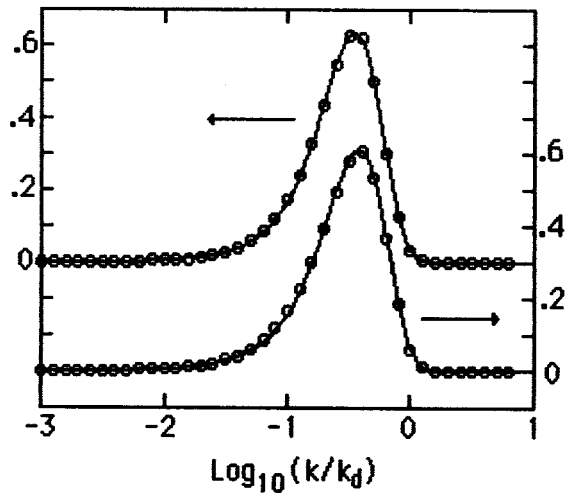

FIG. 3. $kT(k)/\epsilon$ (○○○○) and $2\nu k^3E(k)/\epsilon$ (—) vs $\log_{10}(k/k_d)$ for the optimal solution of (6a). Upper curve: Ko=1.2 and $\eta(k)$ is (10b). Lower curve: Ko=1.5 and $\eta(k)$ is (10a).

$$R_\lambda=\tfrac{2}{3}\sqrt{15}\ \mathrm{Ko}\int_0^{\infty}dx\ F(x)x^n/[x^{n+5/3}+(k_0/k_d)^{n+5/3}]. \tag{12}$$

So long as Ko, n, and R_λ are given, we can use (12) to determine k_0/k_d and then use (11), (5), and some form of $\eta(k)$ to evaluate $T(k)$. By using (2) and (3), we further calculate $D_{LLL}(r)$. Finally, we obtain Figs. 1–10. A detailed account of the numerical procedure will be reported elsewhere.

The finite Reynolds number effect mainly refers to the situation that within the scaling range found in experiments and simulations some small-scale statistics deviate from the prediction of idealized inertial-range models of infinite Reynolds number. A concrete measure of the finite Reynolds number effect depends upon which small-scale property is studied. We choose the third-order structure function $D_{LLL}(r)$ to study the finite Reynolds number effect because there is an exact relationship (1) for $D_{LLL}(r)$ in the inertial range. One may use the deviation of the local scaling exponent $d\log_{10}[D_{LLL}(r)]/d\log_{10}(r)$ from the theoretical value 1 to measure the finite Reynolds number effect. Figures 1 and 2 indicate that the local scaling exponent being unity

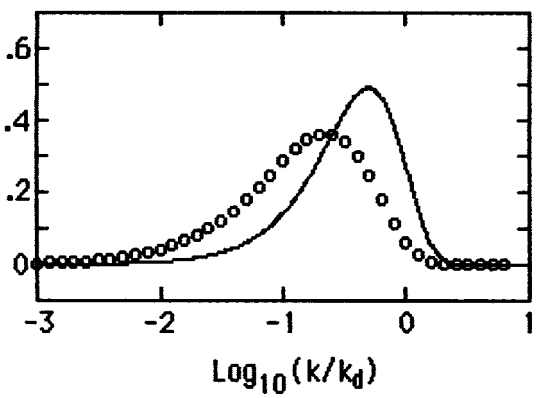

FIG. 4. $kT(k)/\epsilon$ (○○○○) and $2\nu k^3E(k)/\epsilon$ (—) vs $\log_{10}(k/k_d)$ for Pao's formula $F(x)=\exp[-1.5\ \mathrm{Ko}\ x^{4/3}]$, Ko=1.7.

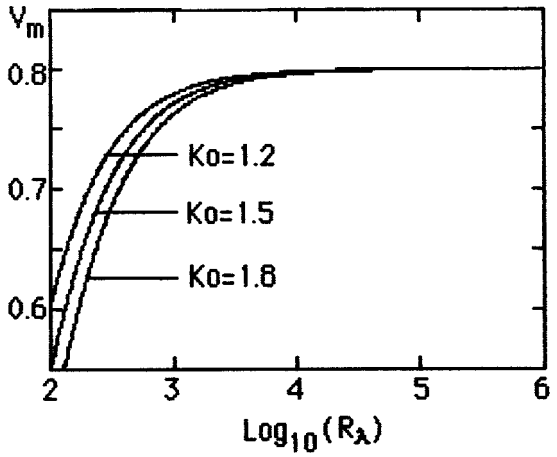

FIG. 5. Maximum value V_m of $-D_{LLL}(r)/\epsilon r$ vs $\log_{10}(R_\lambda)$ for three typical values of Ko. $n=1$ and $\eta(k)$ is (10a).

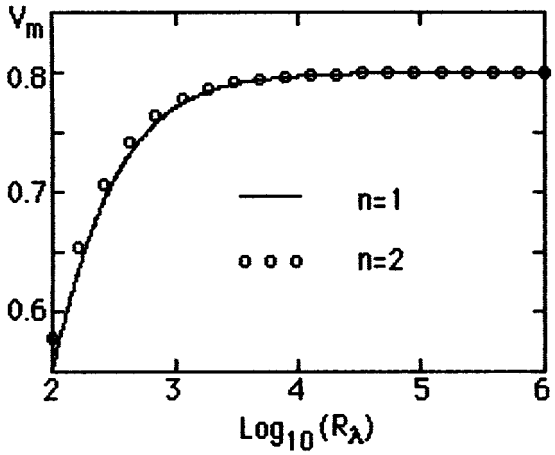

FIG. 7. V_m vs $\log_{10}(R_\lambda)$ for different n. Ko=1.5 and $\eta(k)$ is (10a).

does not imply the validity of the inertial-range relationship (1). Therefore, it is better to measure the finite Reynolds number effect by the equation error of (1), i.e., by the deviation of $-D_{LLL}(r)/\epsilon r$ from the inertial-range value 0.8. In particular, if the maximum value of $-D_{LLL}(r)/\epsilon r$ is smaller than 0.8, then we conclude that there is no inertial range where the finite Reynolds number effect is negligible. The width of the inertial range is

$$W=\log_{10}(r_{\max}/r_{\min}). \tag{13}$$

Here $(r_{\min},r_{\max})$ is the range over which the deviation of $-D_{LLL}(r)/\epsilon r$ from 0.8 is less than the error $\mathcal{E}$. In other words, the finite Reynolds number effect should be less than $\mathcal{E}$ within the inertial range. In our numerical computation, different values of $\mathcal{E}$ are used and compared. Let V_m denote the maximum value of $-D_{LLL}(r)/\epsilon r$. V_m versus $\log_{10}(R_\lambda)$ is given in Fig. 5 for three typical values of the Kolmogorov constant Ko, which show how the finite Reynolds number effect changes with the Reynolds number. Figure 6 gives V_m vs $\log_{10}(R_\lambda)$, while different forms of $\eta(k)$ are used. Figure 7 gives V_m vs $\log_{10}(R_\lambda)$ for different values of the characteristic parameter n in the spectrum (11). Figures 6 and 7 clearly show that different forms of $\eta(k)$ and energy-containing-range spectrum give nearly the same relationship between V_m and $\log_{10}(R_\lambda)$. Figure 8 gives the inertial-range width W against $\log_{10}(R_\lambda)$ for three typical values of Ko, while $\mathcal{E}$=1%. Figure 9 gives W vs $\log_{10}(R_\lambda)$ for three different values of $\mathcal{E}$. From Figs. 1 and 5–9, it is evident that there is no inertial range when $R_\lambda \leqslant 2000$ and R_λ should be higher than 10^4 in order to have an inertial range wider than one decade within which the finite Reynolds number effect is smaller than 1%. One important aspect of the finite Reynolds number effect is how far the anisotropy of the macrostructure penetrates into the small-scale range of finite Reynolds number turbulence. Unfortunately, this cannot be considered here in the framework of isotropic turbulence.

Traditionally, it is believed that one decade of inertial range can be observed in experiments and simulations at $R_\lambda=200$ and more than two decades at $R_\lambda=1500$. Actually, the inertial range observed in experiments and simulations is an approximate $k^{-5/3}$ scaling range in a log-log plot of 1D longitudinal energy spectrum $E_1(k)$ against the wave number k. This approximate $k^{-5/3}$ scaling range is not the same as Kolmogorov's inertial range within which both the viscous effect and the large-scale effect are negligible. From the viewpoint of spectral dynamics [1,6,8], the inertial range is

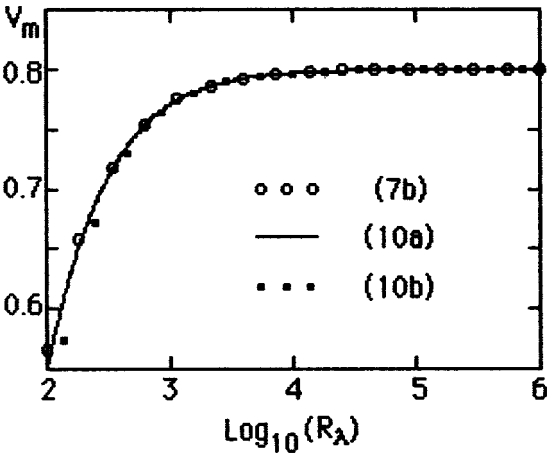

FIG. 6. V_m vs $\log_{10}(R_\lambda)$ for different forms of $\eta(k)$. Ko=1.5 and $n=1$.

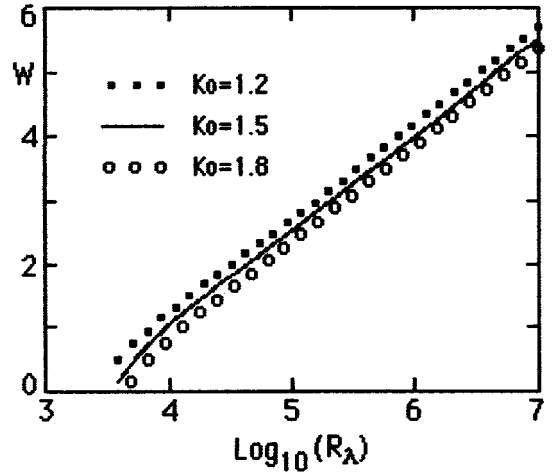

FIG. 8. Inertial-range width W vs $\log_{10}(R_\lambda)$ for three typical values of Ko. $\mathcal{E}$=1%, $n=1$, and $\eta(k)$ is (10a).

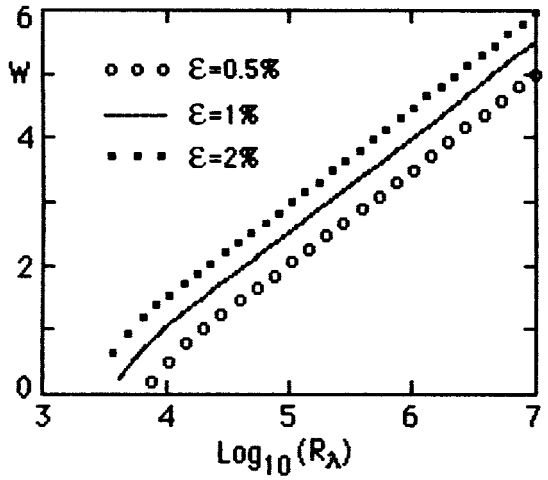

FIG. 9. W vs $\log_{10}(R_\lambda)$ for different $\mathcal{E}$. Ko=1.5, $n=1$, and $\eta(k)$ is (10a).

the wave-number range over which the energy transfer function $\Pi(k)$ is a constant independent of k or the energy transfer spectrum function $T(k)$ is zero. A plot of $kT(k)/\epsilon$ versus $\log_{10}(k/k_d)$ for $R_\lambda=200$, 500, and 1500 is given in Fig. 10, which clearly shows that there is no wave-number range over which $\Pi(k)=$const and $T(k)=0$. Of course, in a log-log plot of $E_1(k)$ versus k for $R_\lambda=200$, 500, and 1500, we can observe an approximate $k^{-5/3}$ scaling range, over which we have

$$E_1(k)/(\epsilon\nu^5)^{1/4}\approx C_1(k/k_d)^{-5/3}.$$

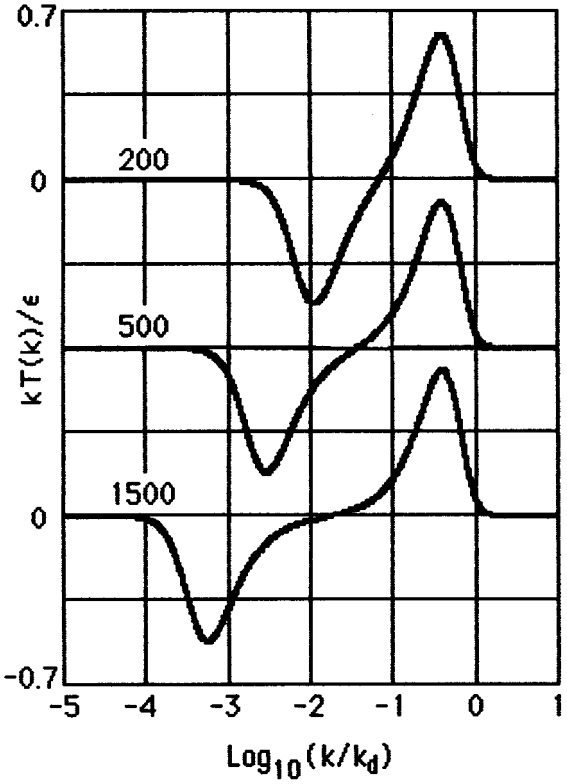

FIG. 10. $kT(k)/\epsilon$ vs $\log_{10}(k/k_d)$ for $R_\lambda=200$, 500, 1500. Ko $=1.5$, $n=1$, and $\eta(k)$ is (10a).

According to Kolmogorov [1], in the inertial range

$$E_1(k)/(\epsilon\nu^5)^{1/4}=\tfrac{18}{55}\mathrm{Ko}(k/k_d)^{-5/3}.$$

It has been shown [11] that C_1 is greater than $\frac{18}{55}$ Ko due to the bump phenomenon related to $T(k)$ not being zero and the Kolmogorov constant $\tilde{K}=\frac{55}{18}C_1$ derived from the $k^{-5/3}$ range observed in experiments and simulations is a pseudo one and is greater than the real Kolmogorov constant Ko. Therefore, over the $k^{-5/3}$ scaling range (which is commonly called the inertial range in experiments and simulations) of $R_\lambda=200$, 500, and 1500, the finite Reynolds number effect has to be considered and is in agreement with the conclusion derived from Figs. 1, 5, and 8 in the preceding paragraph. Another interesting example of the finite Reynolds number effect is that the scaling exponents derived from the scaling range (in a log-log plot of high-order structure functions against r) observed in experiments deviates from the theoretical inertial-range values because the viscous effect is not negligible in the scaling range. Hence Benzi *et al.* [12] suggested plotting high-order structure functions against $D_{LLL}(r)$, instead of plotting high-order structure functions against r, in order to get a better estimation of the scaling exponents.

Most experiments and simulations are at R_λ around 10^2–10^3. The finding that there is no inertial range while $R_\lambda\leqslant 2000$ will have important meaning for the interpretation of the so-called inertial-range data derived from the scaling range observed in experiments and simulations and calls for reexamining the comparison of theories and experiments (or simulations) of the inertial-range statistics. In other words, in the interpretation of these data, the finite Reynolds number effect must be considered. Here we discuss two interesting cases: the interpretation of the experimental data of the third-order structure function $D_{LLL}(r)$ and the experimental support for Kolmogorov's refined similarity hypothesis (RSH). Saddoughi and Veeravalli [4] measure $D_{LLL}(r)$, suppose that Kolmogorov's $\frac{4}{5}$ law (1) is valid over the scaling range caught in their experiments, and then use $\epsilon=-\frac{5}{4}r^{-1}D_{LLL}(r)$ to obtain the energy dissipation rate ϵ. Their experiments are at $R_\lambda=600$–1500 [4]; hence there is no inertial range within which Kolmogorov's $\frac{4}{5}$ law (1) is valid according to Figs. 1 and 5. Over the scaling range found in their experiments at $R_\lambda=600$–1500, $D_{LLL}(r)=-C_3\epsilon r$ is approximately valid; here the constant C_3 is some average value of $-D_{LLL}(r)/\epsilon r$ over the scaling range and is between 0.65 and 0.75 for $R_\lambda=600$–1500 instead of the inertial-range value 0.8 as shown in Fig. 1. As a consequence, the estimation of ϵ by Saddoughi and Veeravalli using $\epsilon=-\frac{5}{4}r^{-1}D_{LLL}(r)$ should be about 10–20 % lower than the real value of ϵ. This might explain why $\epsilon=-\frac{5}{4}r^{-1}D_{LLL}(r)$, experimentally determined by Saddoughi and Veeravalli, is lower than the value estimated from the 1D energy spectra. In the experiments by Zhu, Antonia, and Hosokawa [13], a $D_{LLL}(r)\sim r$ scaling range of about one decade at $R_\lambda=250$ and a scaling range of more than two decades at $R_\lambda=7000$ are observed, the ϵ estimated by 1D energy spectra is used to calculate the constant C_3, and a C_3 smaller than 0.8 is found, consistent with our conclusion. In order to assess Kolmogorov's RSH, recently many authors (see [13] and references therein) have measured the correlation coefficients between Δu_r (or $|\Delta u_r|$) and ϵ_r [or $(r\epsilon_r)^{1/3}$] of high-R_λ turbulence. Here

$\Delta u_r = u(x+r) - u(x)$ is the velocity difference across a distance r and ϵ_r is the local average dissipation over the scale r. A theoretical analysis [14] shows that the experimental data of correlation coefficients are not in agreement with the inertial-range values predicated by Kolmogorov's 1962 (K62) theory. For example, the correlation coefficients

$$\rho_3 = \langle (\Delta u_r - \langle \Delta u_r \rangle)(\epsilon_r - \langle \epsilon_r \rangle) \rangle / (\langle \Delta u_r^2 \rangle \langle \epsilon_r^2 \rangle)^{1/2},$$

$$\rho_4 = \langle (X - \langle X \rangle)(Y - \langle Y \rangle) \rangle / [\langle (X - \langle X \rangle)^2 \rangle \langle (Y - \langle Y \rangle)^2 \rangle]^{1/2},$$

$$X = \Delta u_r, \quad Y = (r \epsilon_r)^{1/3}$$

should be zero in the inertial range according to K62 theory; however, their experimental values in the scaling range observed in experiments (called ''inertial range'' in literature) are regularly positive [13,15]. There are different interpretations for such disagreement between experimental values and theoretical inertial-range values. One possible interpretations is that the disagreement between experimental and theoretical values may related to the finite Reynolds number effect upon the correlation coefficients, which is not known well at present. Since all experimental measurements of correlation coefficients are made at R_λ less than 10^4, according to Figs. 1 and 5–10, the finite Reynolds number effect has to be considered within the scaling range observed in experiments. Only when a detailed understanding of the finite Reynolds number effect has been achieved can we resolve the question of to what extent the experiments and simulations support or deny the RSH of K62 theory. At present we are far from understanding the finite Reynolds number effect. This paper represents a preliminary effort to understand the finite Reynolds number effect in the case of the third-order structure function $D_{LLL}(r)$.

[1] A. S. Monin and A. M. Yaglom, *Statistical Fluid Mechanics* (Cambridge University Press, Cambridge, 1975).
[2] M. Nelkin, Adv. Phys. **43**, 143 (1994); U. Frisch, *Turbulence: The Legacy of A. N. Kolmogorov* (Cambridge University Press, Cambridge, 1995).
[3] H. L. Grant, R. W. Stewart, and A. Moilliet, J. Fluid Mech. **12**, 241 (1962).
[4] S. G. Saddoughi and S. V. Veeravalli, J. Fluid Mech. **268**, 333 (1994).
[5] R. H. Kraichnan, J. Fluid Mech. **5**, 497 (1959); Phys. Fluids **9**, 1728 (1966).
[6] D. C. Leslie, *Developments in the Theory of Turbulence* (Clarendon, Oxford, 1983).
[7] J. R. Herring, D. Schertzer, M. Lesieur, G. R. Newman, J. P. Chollet, and M. Larcheveque, J. Fluid Mech. **124**, 411 (1982).
[8] J. Qian, Phys. Fluids **26**, 2098 (1983); J. Qian, Acta Mech. Sin. **11**, 122 (1995).
[9] J. Qian, Phys. Fluids **27**, 2229 (1984).
[10] D. C. Leslie and G. L. Quarini, J. Fluid Mech. **91**, 65 (1979); J. Qian, Phys. Fluids **29**, 2165 (1986).
[11] J. Qian, J. Phys. Soc. Jpn. **62**, 926 (1993); **65**, 2502 (1996).
[12] R. Benzi, S. Ciliberto, R. Trippicione, C. Baudet, F. Massaioli, and S. Sussi, Phys. Rev. E **48**, R29 (1993); G. Stolovitzky and K. R. Sreenivasan, *ibid*. **48**, R33 (1993).
[13] Y. Zhu, R. A. Antonia, and I. Hosokawa, Phys. Fluids **7**, 1637 (1995).
[14] J. Qian, Phys. Rev. E **54**, 981 (1996).
[15] G. Stolovitzky, P. Kailasnath, and K. R. Sreenivasan, Phys. Rev. Lett. **69**, 1178 (1992).